



Supplement of

Mass changes of the northern Antarctic Peninsula Ice Sheet derived from repeat bi-static synthetic aperture radar acquisitions for the period 2013–2017

Thorsten Seehaus et al.

Correspondence to: Thorsten Seehaus (thorsten.seehaus@fau.de)

The copyright of individual parts of the supplement might differ from the article licence.

1 Evaluation of TanDEM-X elevation measurements

1.1 Comparison to IceBridge data:

The suitability of the processing approach was evaluated using IceBridge IDHDT4 surface elevation change rate (dh/dt) data (Studinger, 2014) from a longer and shifted observation period (2011-2016), which was also employed by Rott et al. (2018) to validate TanDEM-X digital elevation models (DEMs) at the Larsen-B embayment.

The IDHDT4 data covers only limited sections of our study area. Similar to Rott et al. (2018), longitudinal profiles of outlet glaciers were selected, and very crevassed or steep slope areas and regions affected by front position changes were masked out. The IDHDT4 front prints of elevation change measurements represent surface areas of 250x250 m. For the comparison with our TanDEM-X dh/dt fields, the average TanDEM-X dh/dt value within a buffer of 125 m around the center of each IDHDT4 footprint was obtained.

In contrast to Rott et al. (2018), our observation period did not fit the IceBridge IDHDT4 measuring period. Consequently, considerable offsets between TanDEM-X and IDHDT4 dh/dt measurements are revealed at some glaciers with dynamic change rates, like Drygalski, Crane, and Airy-Seller-Flemming (ASF) Glacier. At Drygalski and Crane glaciers, the ice dynamic adjustments due to the ice shelf disintegrations are leading to decreasing dh/dt rates within the IDHDT4 period from 2011-2016 (e.g. for Crane Glacier: -2.318 m/a for 2011-2013 and -0.753 m/a for 2013-2016; Rott et al. (2018)). At ASF Glacier an increasing trend in the surface lowering was revealed several kilometers in-land by Friedl et al. (2018). The trends revealed from both studies fit the discovered offsets between our TanDEM-X and the IDHDT4 dh/dt rates (negative at Drygalski and Crane Glacier, positive at ASF Glacier). Consequently, these glaciers were not considered in the comparison of the elevation change rates from TanDEM-X (2013-2017) and IDHDT4 (2011-2016).

In total 1592 samples were evaluated. In Figure S1 the spatial distribution and the elevation change rate offsets between both datasets are illustrated. The scatter plot in Figure S2 illustrates the concordance of the dh/dt measurements. A positive offset indicates higher surface lowering rates for the IDHDT4 data. A mean offset of 0.12 m/a and a RMSD of 0.337 m/a is obtained. Both values are higher than the findings revealed by Rott et al. (2018) (mean offset of -0.08 m/a and RMSD of 0.20 m/a). However, in contrast to Rott et al. (2018), there is a temporal difference between both dh/dt data sets used in this study, which is most likely explaining the more pronounced differences as compared to Rott et al. (2018). In particular, the offsets in dh/dt in the upper reaches of Leppard and Attlee Glacier lead to some strongly negative offsets (see Figure S1 and S2) and increased RMSD value. These areas of the AP plateau receive higher accumulation rates than the low-lying areas on the east coast (e.g. van Wessem et al., 2015). Subsequently, surface elevations can vary strongly on inter-annual but also sub-annual scales, depending on the accumulation rates and timing of data acquisition. On the other hand differences in the SAR signal penetration between the TanDEM-X acquisitions in 2013 and 2017 can also lead to such offsets (see further below).

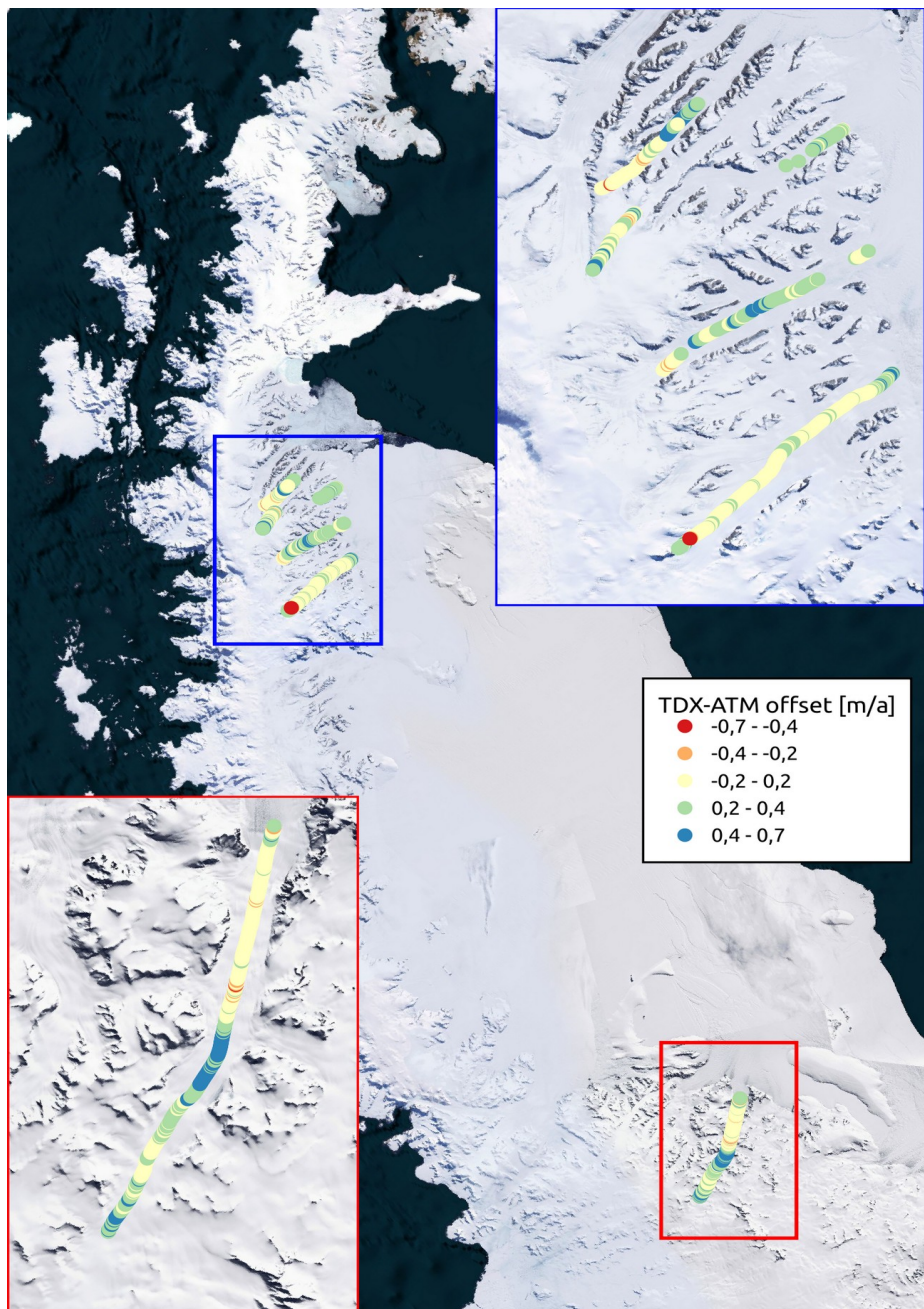


Figure S1: Spatial distribution of the offset between the TanDEM-X elevation change rates and the IceBridge ATM IDHDT4 data. Background: © Microsoft

(c) Microsoft

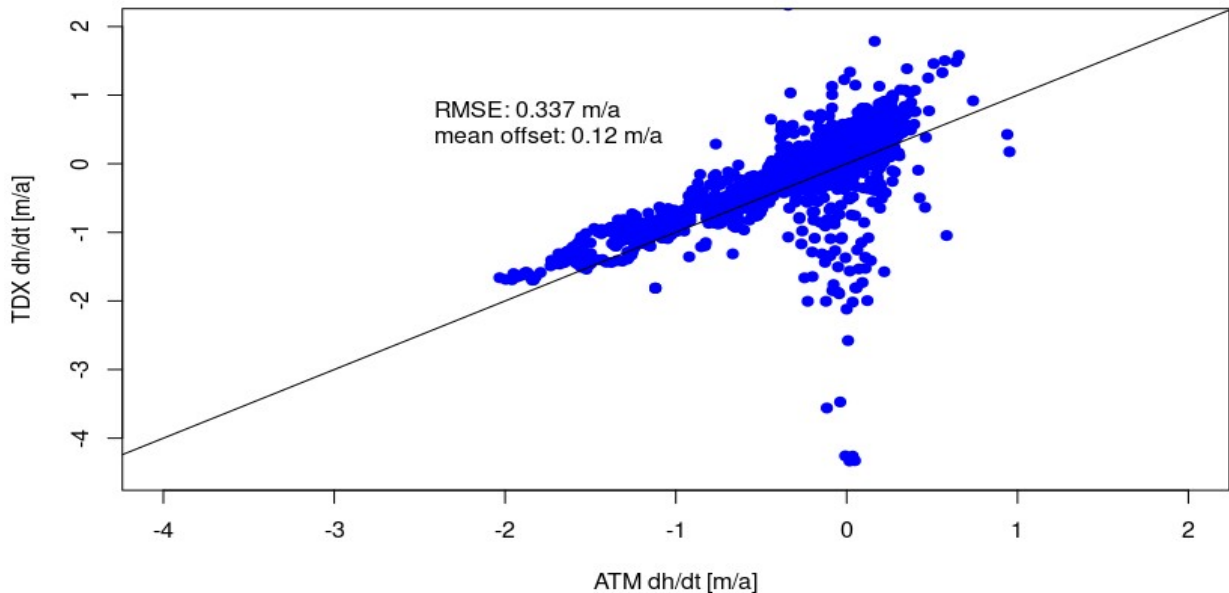


Figure S2: Scatter plot of TanDEM-X (TDX) and IceBridge ATM IDHDT4 elevation change measurements.

1.2 Comparison to REMA:

Contemporaneous time-stamped REMA tiles (Howat et al., 2022) for both TanDEM-X acquisition periods were downloaded at 2 m spatial resolution and bi-linearly resampled to the resolution of the TanDEM-X data (30 m). A temporal offset threshold of 30 days between the individual TanDEM-X acquisitions and the REMA data was applied at pixel level to minimize the impact of surface elevation changes due to temporal offsets. Since the TanDEM-X data was acquired during austral-winter, the amount of available contemporaneous REMA data is quite limited. Subsequently, the provided REMA bitmask was applied to remove unreliable or interpolated information. Only REMA DEM values with bitmask value = 1 were kept. Subsequently, the REMA DEM tiles were horizontally coregistered and vertically corrected for offsets on the rock outcrops (similar to the TanDEM-X raw DEMs, see Section 3 main manuscript). Due to large data gaps and low spatial coverage of the areas used for the coregistration for several REMA tiles, the coregistration did not work and the affected REMA tiles were dismissed. Finally, the remaining REMA tiles and the TanDEM-X DEMs of the respective acquisition periods were differentiated to assess the offset between both surface elevation data sets. The limited availability of REMA data in austral-winter and the coregistration issues led to a limited coverage by elevation difference measurements between the TanDEM-X and REMA data. In Figure S3 the resulting elevation difference map for both TanDEM-X acquisition periods are plotted. The REMA DEM coverages for both periods (2013 and 2017) do not overlap. Consequently, we analyzed each period independently. In Figure S4 the hypsometric distribution of the offsets are illustrated. Negative values indicate that TanDEM-X heights were below the REMA surface, which serves as an indicator for SAR signal penetration. The offsets between REMA and TanDEM-X in 2013 show no trend with elevation, whereas for 2017 a slight trend towards higher offsets in regions above ~1800 m a.s.l. is visible. This finding supports our assumption of a potential SAR signal penetration offset between both acquisitions for elevated regions. (Note: The offsets are measured at different locations and thus SAR signal penetration offset between our TanDEM-X coverage in 2013 and 2017 can not be derived from this data, since the SAR signal penetration can vary strongly on spatial scales, e.g. due to different accumulation rates or melt rates). However, we concluded, that the TanDEM-X and REMA surface

elevations agree quite well (<1 m average offset, which we attribute to SAR signal penetration) for both periods, demonstrating the suitability of our TanDEM-X DEMs as an elevation information source for the study region.

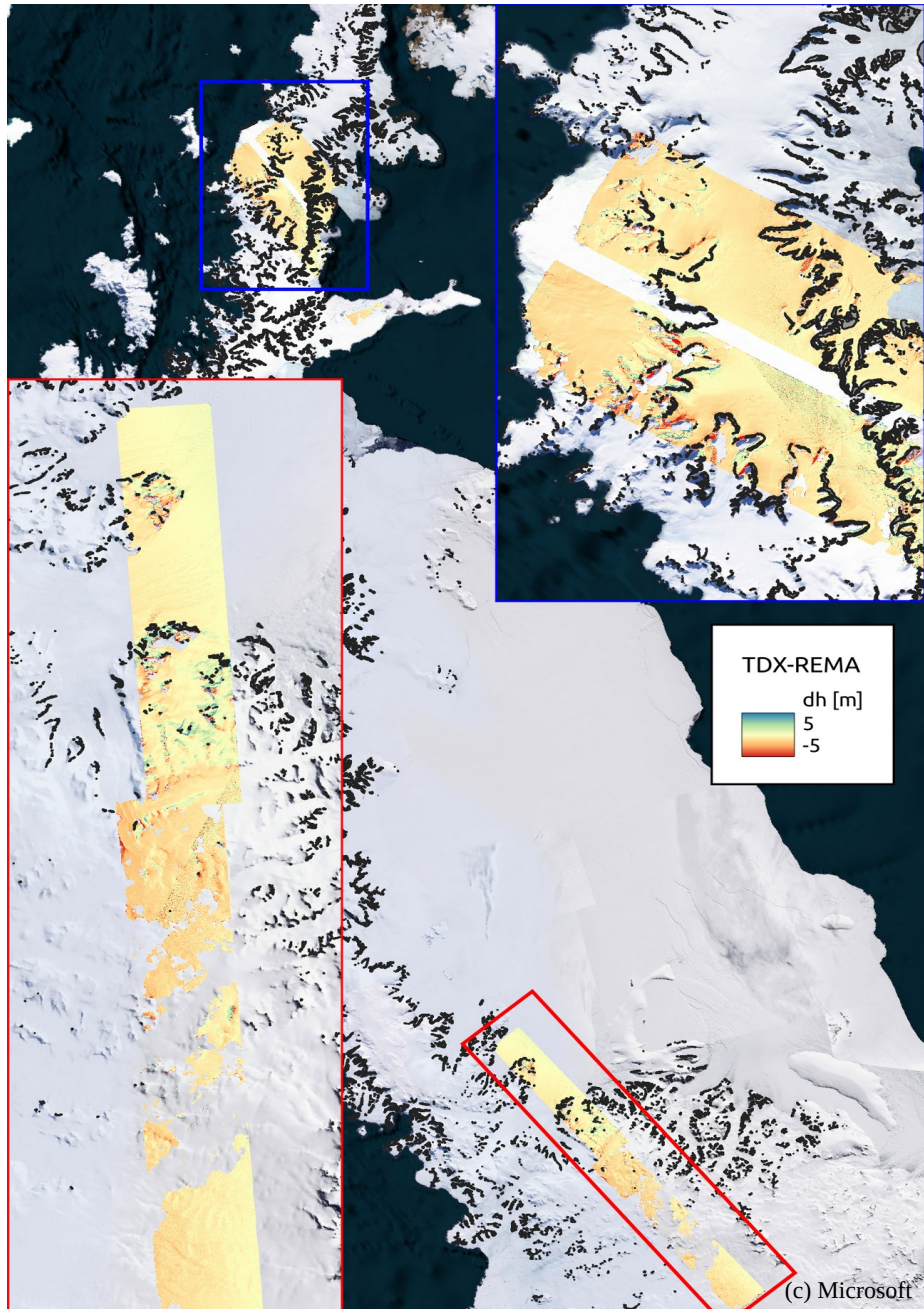


Figure S3: Spatial coverage of elevation differences between contemporaneous TanDEM-X and REMA DEMs for 2013 (blue polygon) and 2017 (red polygon). Background © Microsoft

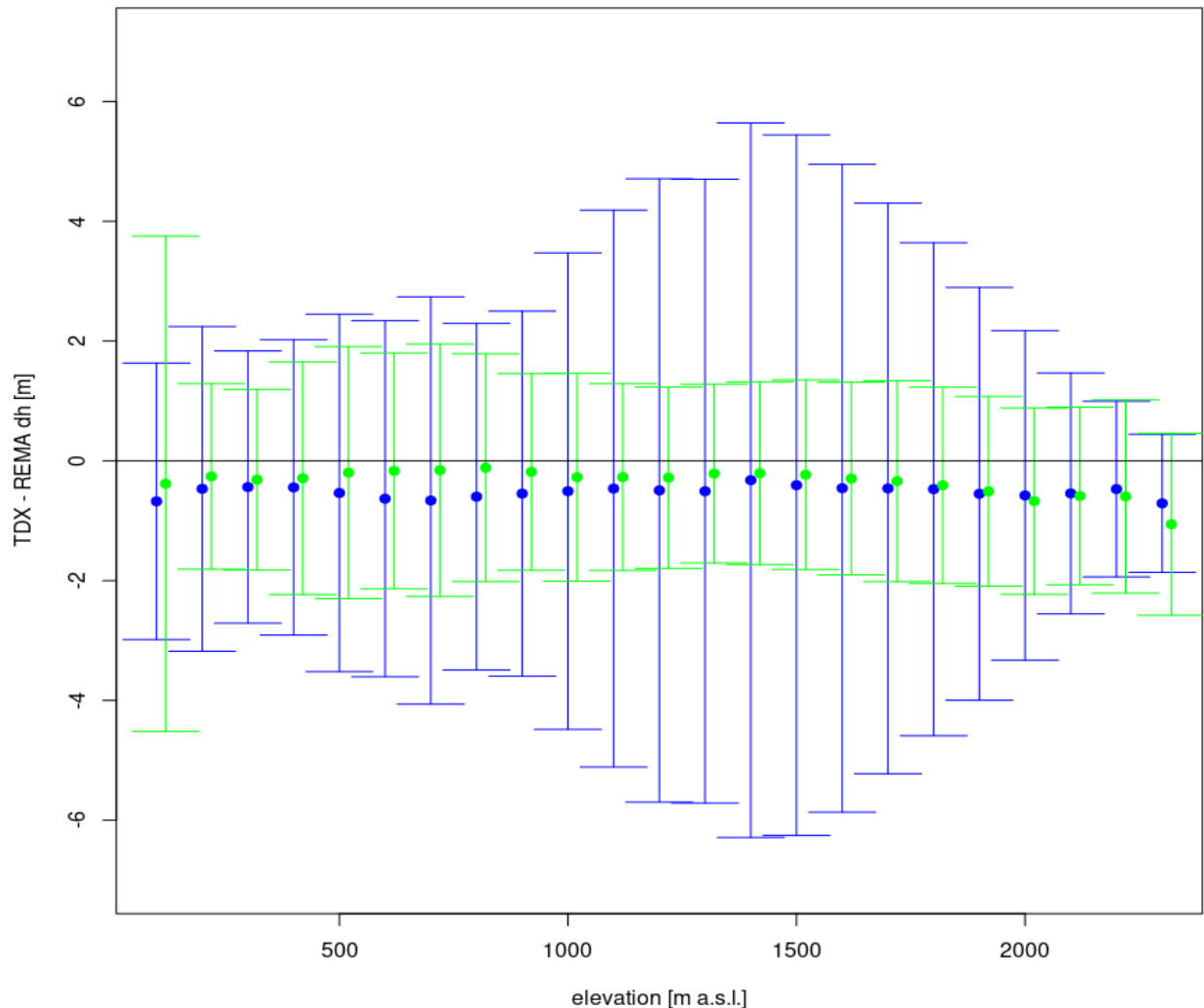


Figure S4: Hypsometric distribution of differences between contemporaneous TanDEM-X and REMA DEMs for 2013 (blue) and 2017 (green). Whiskers indicate root mean square differences (RMSD) for the respective elevation bin

2 SAR backscatter analysis

We carried out an analysis of the SAR backscatter for both TanDEM-X acquisition periods similar to Sommer et al. (2022). The hypsometric distribution of the SAR backscatter values is plotted for both periods in Figure S5. The backscatter values show a similar trend for both periods, with a small average offset of ~1-2 db, and consequently similar backscatter characteristics of the surfaces. However, there is a slight increased offset between the mean values for each elevation bin visible towards higher elevations (**above** ~1800 m a.s.l.). This finding supports our assumption of a potential SAR signal penetration bias at higher elevations.

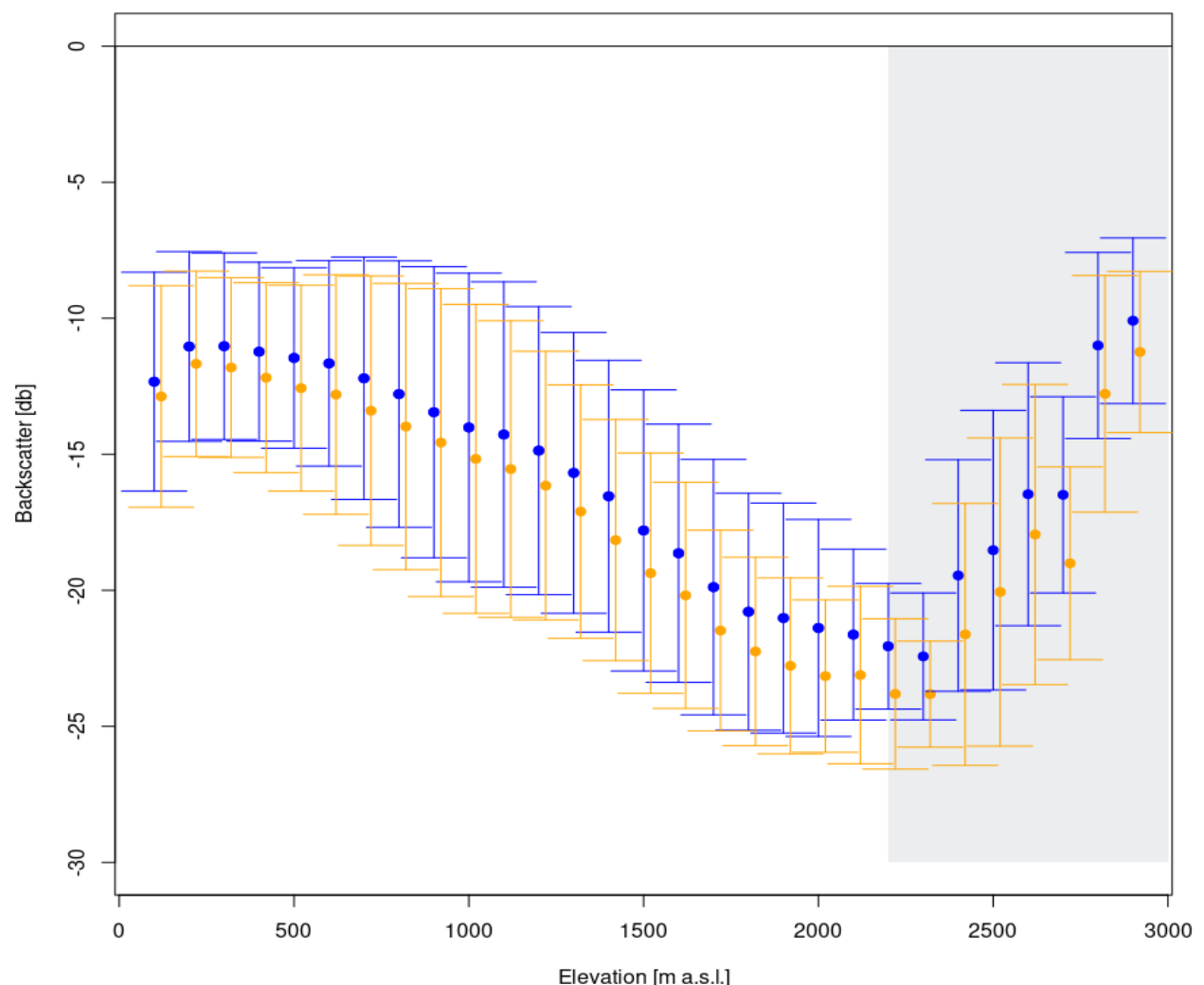


Figure S5: Hypsometric distribution of SAR backscatter values for 2013 (blue) and 2017 (orange). Whiskers indicate normalized mean absolute deviation (NMAD). The gray area marks the upper 1% quantile of the total glacier area distribution (see Figure 3 in the main manuscript)

3 Overview of used TanDEM-X acquisitions

Tables S1: Summary of employed TanDEM-X acquisitions.

Start date & time [YYYYMMDD-hhmmss]	End date & time [YYYYMMDD-hhmmss]	Orbit direction A – ascending D - descending	Rel. orbit number	Beam config. number	Incidence angle [°]	Effective baseline [m]	Height of ambiguity [m]
20130609T082314	20130609T082322	D	125	40	38.51	115.2	-53.2
20130609T082321	20130609T082329	D	125	40	38.55	115.2	-53.3
20130609T082328	20130609T082336	D	125	40	38.55	115.2	-53.4
20130609T082335	20130609T082343	D	125	40	38.48	115.2	-53.5
20130609T082342	20130609T082350	D	125	40	38.56	115.2	-53.8
20130609T082349	20130609T082357	D	125	40	38.58	115.2	-54
20130609T082356	20130609T082404	D	125	40	38.56	115.2	-54.1
20130609T082403	20130609T082411	D	125	40	38.55	115.2	-54.3
20130609T082410	20130609T082418	D	125	40	38.53	115.2	-54.4
20130609T082417	20130609T082425	D	125	40	38.51	115.2	-54.6
20130609T082424	20130609T082432	D	125	40	38.49	115.2	-54.7
20130609T082431	20130609T082439	D	125	40	38.49	115.2	-54.9
20130609T082438	20130609T082446	D	125	40	38.52	115.2	-55.1
20130609T082445	20130609T082453	D	125	40	38.56	115.2	-55.3
20130609T082452	20130609T082500	D	125	40	38.52	115.2	-55.4
20130609T082459	20130609T082507	D	125	40	38.49	115.2	-55.6
20130609T082506	20130609T082514	D	125	40	38.46	115.2	-55.8
20130615T081437	20130615T081445	D	49	60	42.75	124.7	-58.3
20130615T081444	20130615T081452	D	49	60	42.8	124.7	-58.5
20130615T081451	20130615T081459	D	49	60	42.82	124.7	-58.6
20130615T081458	20130615T081506	D	49	60	42.78	124.7	-58.7
20130615T081526	20130615T081534	D	49	60	42.74	124.7	-59.3
20130615T081533	20130615T081541	D	49	60	42.79	124.7	-59.5
20130615T081540	20130615T081548	D	49	60	42.77	124.7	-59.7
20130615T081547	20130615T081555	D	49	60	42.76	124.7	-59.8
20130615T081554	20130615T081602	D	49	60	42.75	124.7	-60
20130615T081601	20130615T081609	D	49	60	42.74	124.7	-60.2
20130615T081608	20130615T081616	D	49	60	42.75	124.7	-60.3
20130615T081615	20130615T081623	D	49	60	42.79	124.7	-60.5
20130615T081622	20130615T081630	D	49	60	42.78	124.7	-60.7
20130615T081629	20130615T081637	D	49	60	42.75	124.7	-60.9
20130615T081636	20130615T081644	D	49	60	42.71	124.7	-61.1
20130620T082322	20130620T082330	D	125	50	40.63	119.2	-56.6
20130620T082329	20130620T082337	D	125	50	40.66	119.2	-56.7
20130620T082336	20130620T082344	D	125	50	40.65	119.2	-56.9
20130620T082343	20130620T082351	D	125	50	40.76	119.2	-57.2
20130620T082350	20130620T082358	D	125	50	40.74	119.2	-57.3
20130620T082357	20130620T082405	D	125	50	40.73	119.2	-57.5
20130620T082404	20130620T082412	D	125	50	40.7	119.2	-57.6
20130620T082411	20130620T082419	D	125	50	40.67	119.2	-57.8
20130620T082418	20130620T082426	D	125	50	40.64	119.2	-57.9
20130620T082425	20130620T082433	D	125	50	40.63	119.2	-58.1
20130620T082432	20130620T082440	D	125	50	40.65	119.2	-58.3
20130620T082439	20130620T082447	D	125	50	40.69	119.2	-58.5
20130620T082446	20130620T082454	D	125	50	40.68	119.2	-58.7
20130620T082453	20130620T082501	D	125	50	40.65	119.2	-58.9
20130620T082500	20130620T082508	D	125	50	40.62	119.2	-59.1
20130620T082507	20130620T082515	D	125	50	40.62	119.2	-59.3

20130621T080724	20130621T080732	D	140	50	40.66	116.6	-58.7
20130621T080731	20130621T080739	D	140	50	40.65	116.6	-58.9
20130621T080738	20130621T080746	D	140	50	40.65	116.6	-59.1
20130621T080745	20130621T080753	D	140	50	40.64	116.6	-59.2
20130621T080752	20130621T080800	D	140	50	40.74	116.6	-59.4
20130621T080759	20130621T080807	D	140	50	40.73	116.6	-59.6
20130625T083241	20130625T083249	D	34	60	42.74	122	-60.8
20130625T083248	20130625T083256	D	34	60	42.73	122	-60.9
20130625T083255	20130625T083303	D	34	60	42.73	122	-61.1
20130625T083302	20130625T083310	D	34	60	42.72	122	-61.3
20130625T083309	20130625T083317	D	34	60	42.72	122	-61.5
20130626T081437	20130626T081445	D	49	40	38.49	118.8	-54.4
20130626T081547	20130626T081555	D	49	40	38.5	114.1	-56.2
20130626T081554	20130626T081602	D	49	40	38.48	114.1	-56.3
20130626T081601	20130626T081609	D	49	40	38.47	114.1	-56.5
20130626T081608	20130626T081616	D	49	40	38.5	114.1	-56.7
20130626T081615	20130626T081623	D	49	40	38.54	114.1	-56.9
20130626T081622	20130626T081630	D	49	40	38.6	114.1	-57.2
20130626T081629	20130626T081637	D	49	40	38.57	114.1	-57.3
20130627T075908	20130627T075916	D	64	60	42.72	119.7	-62.2
20130627T075915	20130627T075923	D	64	60	42.77	119.7	-62.4
20130701T082254	20130701T082259	D	125	40	38.48	119.8	54
20130701T082329	20130701T082337	D	125	60	42.73	120.9	-60.3
20130701T082336	20130701T082344	D	125	60	42.75	120.9	-60.5
20130701T082343	20130701T082351	D	125	60	42.78	120.9	-60.6
20130701T082350	20130701T082358	D	125	60	42.72	120.9	-60.7
20130701T082357	20130701T082405	D	125	60	42.72	120.9	-60.9
20130701T082404	20130701T082412	D	125	60	42.83	120.9	-61.2
20130701T082411	20130701T082419	D	125	60	42.83	120.9	-61.4
20130701T082418	20130701T082426	D	125	60	42.8	120.9	-61.5
20130701T082425	20130701T082433	D	125	60	42.78	120.9	-61.7
20130701T082432	20130701T082440	D	125	60	42.79	120.9	-61.9
20130701T082439	20130701T082447	D	125	60	42.75	120.9	-62.1
20130702T080731	20130702T080739	D	140	60	42.74	119	-62.4
20130702T080738	20130702T080746	D	140	60	42.76	119	-62.7
20130702T080745	20130702T080753	D	140	60	42.74	119	-62.8
20130702T080752	20130702T080800	D	140	60	42.71	119	-62.9
20130702T080759	20130702T080807	D	140	60	42.73	119	-63.1
20130712T082323	20130712T082331	D	125	30	36.28	98.4	-60.8
20130728T083222	20130728T083230	D	34	50	40.68	101.1	-68.3
20130728T083222	20130728T083230	D	34	50	40.68	101.1	-68.3
20130728T083229	20130728T083237	D	34	50	40.66	101.1	-68.4
20130728T083236	20130728T083244	D	34	50	40.65	101.1	-68.5
20130728T083243	20130728T083251	D	34	50	40.67	101.1	-68.5
20130728T083250	20130728T083258	D	34	50	40.69	101.1	-68.7
20130728T083257	20130728T083305	D	34	50	40.66	101.1	-68.7
20130728T083304	20130728T083312	D	34	50	40.63	101.1	-68.8
20130729T081440	20130729T081448	D	49	50	40.64	100.2	-68.6
20130729T081447	20130729T081455	D	49	50	40.63	100.2	-68.6
20130729T081529	20130729T081537	D	49	50	40.67	100.2	-69.2
20130729T081550	20130729T081558	D	49	50	40.62	100.2	-69.4
20130729T081557	20130729T081605	D	49	50	40.59	100.2	-69.5
20130729T081604	20130729T081612	D	49	50	40.58	100.2	-69.6
20130729T081611	20130729T081619	D	49	50	40.6	100.2	-69.7
20130729T081618	20130729T081626	D	49	50	40.66	100.2	-69.8
20130729T081625	20130729T081633	D	49	50	40.69	100.2	-69.9

20130729T081632	20130729T081640	D	49	50	40.67	100.2	-70.1
20130729T081639	20130729T081647	D	49	50	40.62	100.2	-70.2
20130804T080734	20130804T080742	D	140	40	38.46	93.8	-67.3
20130804T080741	20130804T080749	D	140	40	38.45	93.8	-67.4
20130804T080748	20130804T080756	D	140	40	38.52	93.8	-67.6
20130804T080755	20130804T080803	D	140	40	38.55	93.8	-67.7
20140623T083218	20140623T083226	D	34	45	39.33	169.9	-38.6
20140623T083225	20140623T083233	D	34	45	39.31	169.9	-38.7
20140623T083232	20140623T083240	D	34	45	39.3	169.9	-38.8
20140623T083239	20140623T083247	D	34	45	39.28	169.9	-38.8
20140623T083246	20140623T083254	D	34	45	39.27	169.9	-38.9
20140623T083253	20140623T083301	D	34	45	39.26	169.9	-39
20140623T083300	20140623T083308	D	34	45	39.29	169.9	-39.1
20140623T083307	20140623T083315	D	34	45	39.34	169.9	-39.2
20140623T083314	20140623T083322	D	34	45	39.36	169.9	-39.4
20140623T083321	20140623T083329	D	34	45	39.35	169.9	-39.4
20140721T082343	20140721T082350	D	125	65	43.47	162.2	-46.7
20140721T082349	20140721T082357	D	125	65	43.45	162.2	-46.7
20140721T082356	20140721T082404	D	125	65	43.39	162.2	-46.8
20140721T082403	20140721T082411	D	125	65	43.33	162.2	-46.8
20140721T082410	20140721T082418	D	125	65	43.35	162.2	-46.9
20140721T082417	20140721T082425	D	125	65	43.34	162.2	-47
20140721T082424	20140721T082432	D	125	65	43.36	162.2	-47.1
20140721T082431	20140721T082439	D	125	65	43.38	162.2	-47.2
20140721T082438	20140721T082446	D	125	65	43.38	162.2	-47.3
20170514T083249	20170514T083257	D	34	5	30.02	112.9	-41.5
20170514T083256	20170514T083304	D	34	5	30.01	112.9	-41.7
20170514T083303	20170514T083311	D	34	5	30.07	112.9	-41.9
20170519T084148	20170519T084156	D	110	5	30.05	114.9	-42
20170519T084155	20170519T084203	D	110	5	30.05	114.9	-42.2
20170519T084202	20170519T084210	D	110	5	30.08	114.9	-42.4
20170519T084209	20170519T084217	D	110	5	30.11	114.9	-42.7
20170519T084216	20170519T084224	D	110	5	30.04	114.9	-42.8
20170530T084121	20170530T084129	D	110	15	32.52	107.9	-48.3
20170530T084128	20170530T084136	D	110	15	32.49	107.9	-48.5
20170530T084135	20170530T084143	D	110	15	32.51	107.9	-48.7
20170530T084142	20170530T084150	D	110	15	32.56	107.9	-48.9
20170530T084149	20170530T084157	D	110	15	32.55	107.9	-49.2
20170530T084156	20170530T084204	D	110	15	32.49	107.9	-49.4
20170530T084203	20170530T084211	D	110	15	32.52	107.9	-49.7
20170530T084210	20170530T084218	D	110	15	32.49	107.9	-49.9
20170602T235002	20170602T235009	A	165	90	47.82	58.9	-148.7
20170602T235008	20170602T235016	A	165	90	47.82	58.9	-151.1
20170602T235015	20170602T235018	A	165	90	47.84	58.9	-152.6
20170605T083215	20170605T083223	D	34	15	32.49	114.6	-43.7
20170605T083222	20170605T083230	D	34	15	32.55	114.6	-44
20170605T083229	20170605T083237	D	34	15	32.52	114.6	-44.2
20170605T083236	20170605T083244	D	34	15	32.45	114.6	-44.4
20170605T083243	20170605T083251	D	34	15	32.47	114.6	-44.7
20170605T083250	20170605T083258	D	34	15	32.49	114.6	-45
20170605T083257	20170605T083305	D	34	15	32.48	114.6	-45.2
20170605T083304	20170605T083312	D	34	15	32.49	114.6	-45.5
20170605T083311	20170605T083319	D	34	15	32.48	114.6	-45.8
20170605T083318	20170605T083326	D	34	15	32.47	114.6	-46
20170605T083325	20170605T083333	D	34	15	32.47	114.6	-46.3
20170605T083332	20170605T083340	D	34	15	32.46	114.6	-46.5

20170605T083339	20170605T083347	D	34	15	32.51	114.6	-46.9
20170605T083346	20170605T083354	D	34	15	32.48	114.6	-47.1
20170605T083353	20170605T083401	D	34	15	32.49	114.6	-47.5
20170605T083400	20170605T083408	D	34	15	32.45	114.6	-47.7
20170606T081624	20170606T081632	D	49	25	34.83	113.5	-49.5
20170606T081631	20170606T081639	D	49	25	34.84	113.5	-49.8
20170606T081638	20170606T081646	D	49	25	34.89	113.5	-50.1
20170606T081645	20170606T081653	D	49	25	34.99	113.5	-50.5
20170606T081652	20170606T081700	D	49	25	34.95	113.5	-50.7
20170606T081659	20170606T081707	D	49	25	34.93	113.5	-51
20170609T232430	20170609T232437	A	104	20	33.84	16.6	-346.1
20170611T082331	20170611T082339	D	125	15	32.48	115	-43.5
20170611T082338	20170611T082346	D	125	15	32.48	115	-43.7
20170611T082455	20170611T082503	D	125	15	32.45	115	-46.5
20170611T082502	20170611T082510	D	125	15	32.46	115	-46.8
20170611T082509	20170611T082517	D	125	15	32.52	115	-47.1
20170611T082516	20170611T082524	D	125	15	32.55	115	-47.4
20170611T082523	20170611T082531	D	125	15	32.47	115	-47.6
20170611T082530	20170611T082535	D	125	15	32.44	115	-47.8
20170613T234954	20170613T235002	A	165	40	38.46	32.9	-201.3
20170613T235001	20170613T235006	A	165	40	38.49	32.9	-207
20170616T083223	20170616T083231	D	34	25	34.86	126.1	-43.7
20170616T083230	20170616T083238	D	34	25	34.88	126.1	-44
20170616T083237	20170616T083245	D	34	25	34.9	126.1	-44.2
20170616T083244	20170616T083252	D	34	25	34.88	126.1	-44.5
20170616T083251	20170616T083259	D	34	25	34.89	126.1	-44.8
20170616T083258	20170616T083306	D	34	25	34.87	126.1	-45
20170616T083305	20170616T083313	D	34	25	34.87	126.1	-45.3
20170616T083312	20170616T083320	D	34	25	34.86	126.1	-45.6
20170616T083319	20170616T083327	D	34	25	34.85	126.1	-45.9
20170616T083326	20170616T083334	D	34	25	34.87	126.1	-46.2
20170616T083333	20170616T083341	D	34	25	34.91	126.1	-46.5
20170616T083340	20170616T083348	D	34	25	34.9	126.1	-46.8
20170616T083347	20170616T083355	D	34	25	34.89	126.1	-47.2
20170621T084114	20170621T084122	D	110	25	34.91	128.2	-44.2
20170621T084121	20170621T084129	D	110	25	34.87	128.2	-44.5
20170621T084128	20170621T084136	D	110	25	34.86	128.2	-44.7
20170621T084135	20170621T084143	D	110	25	34.86	128.2	-45
20170621T084142	20170621T084150	D	110	25	34.83	128.2	-45.2
20170621T084149	20170621T084157	D	110	25	34.86	128.2	-45.6
20170621T084156	20170621T084204	D	110	25	34.9	128.2	-45.9
20170622T082332	20170622T082340	D	125	25	34.9	126.8	-43.1
20170622T082339	20170622T082347	D	125	25	34.88	126.8	-43.3
20170622T082346	20170622T082354	D	125	25	34.86	126.8	-43.6
20170622T082353	20170622T082401	D	125	25	34.84	126.8	-43.8
20170622T082400	20170622T082408	D	125	25	34.91	126.8	-44.1
20170622T082407	20170622T082415	D	125	25	34.9	126.8	-44.4
20170622T082414	20170622T082422	D	125	25	34.9	126.8	-44.7
20170622T082421	20170622T082429	D	125	25	34.89	126.8	-44.9
20170622T082428	20170622T082436	D	125	25	34.88	126.8	-45.2
20170622T082435	20170622T082443	D	125	25	34.86	126.8	-45.5
20170622T082442	20170622T082450	D	125	25	34.85	126.8	-45.7
20170622T082449	20170622T082457	D	125	25	34.84	126.8	-46
20170622T082456	20170622T082504	D	125	25	34.84	126.8	-46.3
20170622T082503	20170622T082511	D	125	25	34.86	126.8	-46.7
20170622T082510	20170622T082518	D	125	25	34.92	126.8	-47

20170622T082517	20170622T082525	D	125	25	34.86	126.8	-47.2
20170624T234952	20170624T234956	A	165	75	45.18	39.2	-200.9
20170624T234955	20170624T235003	A	165	75	45.2	39.2	-205.4
20170624T235002	20170624T235010	A	165	75	45.22	39.2	-212.3
20170624T235009	20170624T235015	A	165	75	45.23	39.2	-218.5
20170625T233259	20170625T233302	A	13	40	38.42	13.7	-513.6
20170625T233301	20170625T233309	A	13	40	38.49	13.7	-546.4
20170625T233308	20170625T233315	A	13	40	38.49	13.7	-627.7
20170626T231559	20170626T231602	A	28	3	21.4	34.7	97.9
20170626T231600	20170626T231608	A	28	3	21.38	34.7	95.2
20170626T231605	20170626T231608	A	28	3	21.37	34.7	93.2
20170627T083230	20170627T083238	D	34	35	37.12	140.4	-43.8
20170627T083237	20170627T083245	D	34	35	37.17	140.4	-44.1
20170627T083244	20170627T083252	D	34	35	37.21	140.4	-44.3
20170627T083408	20170627T083416	D	34	15	32.51	118.9	-43
20170628T081502	20170628T081510	D	49	35	37.15	142.5	-43.3
20170630T234131	20170630T234139	A	89	70	44.57	29.8	-274.9
20170630T234138	20170630T234146	A	89	70	44.58	29.8	-289.2
20170630T234144	20170630T234147	A	89	70	44.59	29.8	-294.8
20170703T082339	20170703T082347	D	125	35	37.15	141	-43.2
20170703T082346	20170703T082354	D	125	35	37.18	141	-43.5
20170703T082353	20170703T082401	D	125	35	37.16	141	-43.8
20170703T082524	20170703T082532	D	125	25	34.85	122.7	-45.1
20170703T082531	20170703T082539	D	125	25	34.87	122.7	-45.5
20170706T233301	20170706T233304	A	13	40	38.43	37.6	-168.7
20170706T233302	20170706T233310	A	13	40	38.49	37.6	-170.2
20170706T233309	20170706T233316	A	13	40	38.5	37.6	-173.4
20170708T083357	20170708T083403	D	34	25	34.85	80.7	-69.6
20170708T083402	20170708T083410	D	34	25	34.84	80.7	-69.8
20170708T083409	20170708T083417	D	34	25	34.86	80.7	-70.1
20170709T081626	20170709T081634	D	49	10	31.37	75.7	-64.5
20170709T081633	20170709T081641	D	49	10	31.37	75.7	-64.8
20170709T081640	20170709T081648	D	49	10	31.31	75.7	-64.9
20170709T081647	20170709T081655	D	49	10	31.39	75.7	-65.2
20170714T082333	20170714T082341	D	125	10	31.37	81.1	-61.6
20170716T235004	20170716T235011	A	165	90	47.82	55.5	-157.6
20170716T235010	20170716T235018	A	165	90	47.83	55.5	-159.5
20170716T235016	20170716T235019	A	165	90	47.84	55.5	-160.7
20170717T233302	20170717T233310	A	13	25	34.89	28.6	-198.1
20170717T233309	20170717T233317	A	13	25	34.91	28.6	-203.5
20170717T233315	20170717T233318	A	13	25	34.89	28.6	-206.6
20170718T231555	20170718T231602	A	28	6	28.75	15.8	-284.1
20170718T231601	20170718T231609	A	28	6	28.77	15.8	-298.3
20170719T083217	20170719T083225	D	34	10	31.35	82	-58.5
20170719T083224	20170719T083232	D	34	10	31.37	82	-58.7
20170719T083231	20170719T083239	D	34	10	31.32	82	-58.9
20170719T083238	20170719T083246	D	34	10	31.27	82	-59.1
20170719T083245	20170719T083253	D	34	10	31.35	82	-59.4
20170719T083252	20170719T083300	D	34	10	31.38	82	-59.7
20170719T083259	20170719T083307	D	34	10	31.38	82	-59.9
20170720T081612	20170720T081620	D	49	30	36.19	87.1	-67.6
20170720T081619	20170720T081627	D	49	30	36.19	87.1	-67.8
20170720T081626	20170720T081634	D	49	30	36.18	87.1	-68.1
20170720T081633	20170720T081641	D	49	30	36.2	87.1	-68.3
20170720T081640	20170720T081648	D	49	30	36.24	87.1	-68.6
20170720T081647	20170720T081655	D	49	30	36.33	87.1	-68.9

20170720T081654	20170720T081702	D	49	30	36.26	87.1	-69
20170720T081701	20170720T081709	D	49	30	36.26	87.1	-69.3
20170722T234129	20170722T234134	A	89	90	47.81	52.9	-164.8
20170722T234133	20170722T234141	A	89	90	47.82	52.9	-166.7
20170724T084151	20170724T084159	D	110	30	36.21	88.6	-66.6
20170724T084158	20170724T084206	D	110	30	36.21	88.6	-66.8
20170724T084205	20170724T084213	D	110	30	36.24	88.6	-67.1
20170727T234956	20170727T235004	A	165	40	38.46	38	-171.3
20170727T235003	20170727T235008	A	165	40	38.49	38	-174
20170730T083225	20170730T083233	D	34	30	36.21	97	-61.3
20170730T083232	20170730T083240	D	34	30	36.23	97	-61.6
20170730T083239	20170730T083247	D	34	30	36.27	97	-61.9
20170730T083246	20170730T083254	D	34	30	36.28	97	-62.1
20170730T083253	20170730T083301	D	34	30	36.28	97	-62.4
20170730T083300	20170730T083308	D	34	30	36.27	97	-62.6
20170730T083307	20170730T083315	D	34	30	36.23	97	-62.9
20170730T083314	20170730T083322	D	34	30	36.19	97	-63.1
20170801T235826	20170801T235834	A	74	65	43.41	42.2	-182.6
20170802T234128	20170802T234134	A	89	35	37.15	27.1	-221.1
20170802T234133	20170802T234141	A	89	35	37.18	27.1	-227.4
20170802T234140	20170802T234147	A	89	35	37.2	27.1	-234.9
20170810T083240	20170810T083248	D	34	40	38.45	104.8	61.7
20170810T083247	20170810T083255	D	34	40	38.48	104.8	62
20170811T081628	20170811T081636	D	49	20	33.83	91.5	-58.2
20170811T081635	20170811T081643	D	49	20	33.83	91.5	-58.5
20170811T081642	20170811T081650	D	49	20	33.85	91.5	-58.9
20170811T081649	20170811T081657	D	49	20	33.94	91.5	-59.3
20170815T084124	20170815T084132	D	110	10	31.38	93.3	-52.1
20170815T084131	20170815T084139	D	110	10	31.45	93.3	-52.5
20170815T084138	20170815T084146	D	110	10	31.4	93.3	-52.8
20170815T084145	20170815T084153	D	110	10	31.45	93.3	-53.1
20170816T082459	20170816T082507	D	125	30	36.22	95.3	-61.2
20170816T082506	20170816T082514	D	125	30	36.23	95.3	-61.5
20170816T082513	20170816T082521	D	125	30	36.27	95.3	-61.9
20170816T082520	20170816T082528	D	125	30	36.24	95.3	-62.1
20170816T082527	20170816T082535	D	125	30	36.24	95.3	-62.5
20170816T082534	20170816T082542	D	125	30	36.25	95.3	-62.9
20170816T082541	20170816T082549	D	125	30	36.27	95.3	-63.4

4 References

- Friedl, P., Seehaus, T.C., Wendt, A., Braun, M.H., Höppner, K., 2018. Recent dynamic changes on Fleming Glacier after the disintegration of Wordie Ice Shelf, Antarctic Peninsula. *The Cryosphere* 12, 1347–1365. <https://doi.org/10.5194/tc-12-1347-2018>
- Howat, I., Porter, C., Noh, M.-J., Husby, E., Khuvis, S., Danish, E., Tomko, K., Gardiner, J., Negrete, A., Yadav, B., Klassen, J., Kelleher, C., Cloutier, M., Bakker, J., Enos, J., Arnold, G., Bauer, G., Morin, P., 2022. The Reference Elevation Model of Antarctica - Strips, Version 4.1. <https://doi.org/10.7910/DVN/X7NDNY>
- Rott, H., Abdel Jaber, W., Wuite, J., Scheiblauer, S., Floricioiu, D., van Wessem, J.M., Nagler, T., Miranda, N., van den Broeke, M.R., 2018. Changing pattern of ice flow and mass balance for glaciers discharging into the Larsen A and B embayments, Antarctic Peninsula, 2011 to 2016. *The Cryosphere* 12, 1273–1291. <https://doi.org/10.5194/tc-12-1273-2018>
- Sommer, C., Seehaus, T., Glazovsky, A., Braun, M.H., 2022. Brief communication: Increased glacier mass loss in the Russian High Arctic (2010–2017). *The Cryosphere* 16, 35–42. <https://doi.org/10.5194/tc-16-35-2022>
- Studinger, M., 2014. IceBridge ATM L4 Surface Elevation Rate of Change, Version 1. <https://doi.org/10.5067/BCW6CI3TXOCY>
- van Wessem, J.M., Ligtenberg, S.R.M., Reijmer, C.H., van de Berg, W.J., van den Broeke, M.R., Barrand, N.E., Thomas, E.R., Turner, J., Wuite, J., Scambos, T.A., van Meijgaard, E., 2015. The modelled surface mass balance of the Antarctic Peninsula at 5.5 km horizontal resolution. *The Cryosphere Discuss.* 9, 5097–5136. <https://doi.org/10.5194/tcd-9-5097-2015>